



Application of MRI-Based Radiomics in Preoperative Prediction of *NF2* Alteration in Intracranial Meningiomas

OPEN ACCESS

Edited by:

Ian Dunn,
University of Oklahoma Health
Sciences Center, United States

Reviewed by:

Guoping Li,
Harvard Medical School, United States
Xiaohua Qian,
Shanghai Jiao Tong University, China

*Correspondence:

Ye Gong
drgongye@163.com

Specialty section:

This article was submitted to
Neuro-Oncology and
Neurosurgical Oncology,
a section of the journal
Frontiers in Oncology

Received: 19 February 2022

Accepted: 06 June 2022

Published: 28 September 2022

Citation:

Sun S, Ren L, Miao Z,
Hua L, Wang D, Deng J,
Chen J, Liu N and Gong Y
(2022) Application of MRI-Based
Radiomics in Preoperative
Prediction of *NF2* Alteration
in Intracranial Meningiomas.
Front. Oncol. 12:879528.
doi: 10.3389/fonc.2022.879528

Shuchen Sun^{1,2,3}, Leihao Ren^{1,2,3}, Zong Miao⁴, Lingyang Hua^{1,2,3}, Dajun Wang^{1,2,3},
Jiaojiao Deng^{1,2,3}, Jiawei Chen^{1,2,3}, Ning Liu⁴ and Ye Gong^{1,2,3,5*}

¹ Department of Neurosurgery, Huashan Hospital, Fudan University, Shanghai, China, ² Institute of Neurosurgery, Fudan University, Shanghai, China, ³ Shanghai Key Laboratory of Brain Function Restoration and Neural Regeneration, Shanghai, China, ⁴ Department of Neurosurgery, Changhai Hospital, Naval Medical University (Second Military Medical University), Shanghai, China, ⁵ Department of Critical Care Medicine, Huashan Hospital, Fudan University, Shanghai, China

Purpose: This study aimed to investigate the feasibility of predicting *NF2* mutation status based on the MR radiomic analysis in patients with intracranial meningioma.

Methods: This retrospective study included 105 patients with meningiomas, including 60 *NF2*-mutant samples and 45 wild-type samples. Radiomic features were extracted from magnetic resonance imaging scans, including T1-weighted, T2-weighted, and contrast T1-weighted images. Student's t-test and LASSO regression were performed to select the radiomic features. All patients were randomly divided into training and validation cohorts in a 7:3 ratio. Five linear models (RF, SVM, LR, KNN, and xgboost) were trained to predict the *NF2* mutational status. Receiver operating characteristic curve and precision-recall analyses were used to evaluate the model performance. Student's t-tests were then used to compare the posterior probabilities of *NF2* mut/loss prediction for patients with different *NF2* statuses.

Results: Nine features had nonzero coefficients in the LASSO regression model. No significant differences was observed in the clinical features. Nine features showed significant differences in patients with different *NF2* statuses. Among all machine learning algorithms, SVM showed the best performance. The area under curve and accuracy of the predictive model were 0.85; the F1-score of the precision-recall curve was 0.80. The model risk was assessed by plotting calibration curves. The p-value for the H-L

goodness of fit test was 0.411 ($p > 0.05$), which indicated that the difference between the obtained model and the perfect model was statistically insignificant. The AUC of our model in external validation was 0.83.

Conclusion: A combination of radiomic analysis and machine learning showed potential clinical utility in the prediction of preoperative NF2 status. These findings could aid in developing customized neurosurgery plans and meningioma management strategies before postoperative pathology.

Keywords: meningioma, radiomics, NF2, machine learning, SVM - support vector machine

INTRODUCTION

Meningioma is the most common primary tumor of the central nervous system (CNS), accounting for approximately 26.1-38.3% of all intracranial tumors (1-3). According to the WHO CNS tumor grading criterion, meningiomas are categorized into three grades and 15 histological subtypes based solely on the morphological features of the tumor cells. Despite the widespread use of the WHO classification, it fails to accurately predict the clinical behavior, aggressiveness, and recurrence of particular tumors. With the deeper understanding of the molecular landscape of meningioma, in addition to the histological diagnosis, the newest 2021 CNS tumor diagnostic criterion began to integrate the molecular and genetic profiling to assist in diagnoses and evaluate prognosis.

The *NF2* gene was first implicated in meningiomas after it was found that its inactivation resulted in the genetic tumor predisposition syndrome of neurofibromatosis type 2. *NF2* is a tumor suppressor gene comprised of 17 exons with 2 splicing isoforms that is positioned on chromosome 22q12.2 (4). Alterations in the *NF2* gene, which can be caused by mutation, allelic inactivation, splicing alterations, or Chromosome 22 loss, have been implicated in approximately 30-60% of sporadic meningiomas, making it the single most frequent gene alteration in this tumor (5). The frequency of *NF2* mutations is similar in WHO Grade 1, 2 and 3 grades. However, it varies among histological subtypes and locations and are more likely to be observed in atypical and cerebral hemispheres. *NF2* gene inactivation is considered to play a significant role in the development of meningiomas (5, 6). Patients with *NF2* mutations were also reported to show worse outcomes (7). Clinical trials targeting *NF2* has been under way (NCT02523014). Thus, prediction of the *NF2* status before surgery can aid in the development of personalized treatment strategies for meningioma patients.

Radiomics is a novel practice in the field of machine learning. It could be used to extract and analyze medical imaging data (8). By conversion of sparse magnetic resonance imaging (MRI) into data, an immense amount of imaging information that is otherwise invisible to the naked eye in multiple dimensions could be generated (9). Radiomics is a potential approach for noninvasive high-throughput mining of tumor characteristics and has been applied in several other intracranial tumors, including glioma and schwannoma (10, 11). For meningiomas,

algorithms have been developed in previous studies to predict WHO grade, tumor texture, peritumoral edema, and Ki-67 labels through radiomics. These models reported good performance in terms of accuracy and sensitivity (12-14). The status of well-known genetic changes could be accurately predicted by radiomics in several CNS tumors. However, such studies were scarcely mentioned in meningiomas (15, 16).

In this study, we investigated the utility of a radiomics signature based on multiparametric MRI as a preoperative and noninvasive biomarker of *NF2* status in meningiomas.

MATERIALS AND METHODS

Patients

A total of 105 meningioma patients underwent surgical resections between 2019 and 2021 at Huashan Neurosurgical Center were enrolled. Histological diagnoses were reviewed according to 2016 WHO meningioma grading criteria by two experienced neuropathologists (Dr. H.C and Dr. HX.C). Clinical information including age, gender, location, treatment status, the extent of resection, surgical outcome, and neurological functions was extracted from the medical records. Patients with recurrent meningioma who underwent another operation to remove the recurrent tumor were considered as recurrent meningioma cases. Patients with multiple meningiomas were also recorded. The clinical data of 105 patients was shown in.

Table 1 30 meningioma patients from First Affiliated Hospital of Nanjing Medical University were enrolled as External verification. The clinical data of 30 patients are shown in **Supplementary Material 1**. The specific research process of this study is shown in **Figure 1**. This study was approved by the Human Subjects Institutional Review Board of Huashan Hospital, Fudan University.

Next Generation Sequencing

Bidirectional sequencing was performed to detect microlesions in the *NF2* gene. DNA was extracted from tumor tissue with TIANamp Genomic DNA Kit (Tiangen Biotech, Beijing, China) as instructed by the manufacturers. The whole coding sequence and the exon-intron boundaries of the gene were amplified by a standard polymerase chain reaction (PCR). Subsequently, the product was used for bidirectional sequencing, as described previously (17). The sequence data were analyzed by Sequencer

TABLE 1 | Clinical data of enrolled patients.

| | NF2 mut/loss (60) | NF2 wild (45) | All (105) | P |
|-------------------------|-------------------------|------------------------|-------------------------|-------|
| Age | 54.10 ± 9.90 | 51.93 ± 9.14 | 53.17 ± 9.60 | 0.254 |
| Female/Male | 2:33 | 2:21 | 2:28 | 1.00 |
| WHO grade | | | | |
| WHO grade 1 | 50 (64.29%) | 40 (13.21%) | 90 | 0.47 |
| WHO grade 2 | 9 (28.57%) | 5 (79.25%) | 14 | |
| WHO grade 3 | 1 (4.08%) | 0 (7.55%) | 1 | |
| Location | | | | |
| Skull base | 20 (33.33%) | 25 (55.56%) | 45 (42.86%) | 0.07 |
| Convexity | 14 (23.33%) | 7 (15.56%) | 21 (20.00%) | |
| Parasagittal | 26 (43.33%) | 13 (28.89%) | 39 (37.14%) | |
| Multiple | 3 | 0 | 3 | 0.258 |
| Recurrent | 12 | 4 | 16 | 0.170 |
| Ki-67 labeling index(%) | 4.10 ± 2.70 (range1-12) | 3.67 ± 1.94 (range1-8) | 3.91 ± 2.40 (range1-12) | 0.341 |
| PR positive | 46 (76.67%) | 40 (88.89%) | 86 (81.9%) | 0.130 |
| H3K27me3 positive | 51 (85.00%) | 39 (86.67%) | 91 (86.7%) | 0.773 |

4.9 (Genecode, MI, USA) and compared with the *NF2* sequence (NM_016418) from GenBank. Mutations were described according to the standard nomenclature for DNA sequence changes according to the Human Genome Variation Society (HGVS).

Loss of Heterozygosity Analysis of 22q

Each tumor sample was subjected to PCR analysis. A fraction of the PCR product (0.5 liters) was mixed with 0.1 liters of Genescan 500 size standard (PE Applied Biosystems Foster City, CA, USA) and 0.9 liters of formamide loading buffer. Combinations were electrophoresed on a 5 percent polyacrylamide gels on an ABI 377 DNA sequencer (PE Applied Biosystems Foster city CA, USA) for 2 hours after being denaturated at 96°C for 5 minutes. Individual gel lanes were visualized using the Genotype 2.0 software. The samples were scored using strict criteria. The two highest peaks within the predicted size range were designated as alleles. A loss of heterozygosity was defined as a ratio of T1:T2/N1:N2 of less than 0.67 or more than 1.50. The majority of normal DNA amplifications yielded two PCR results, showing heterozygosity. The ratio of allelic loss to informative instances was used to calculate the LOH frequency of a locus. The average LOH frequency of the long arm of chromosome 22 was the sum of the LOH frequencies of each location.

Immunohistochemistry

Immunohistochemical staining was performed using monoclonal antibodies against Ki-67 [Signalway (SAB), Shanghai, China; 1:200 dilution]. The cells stained in immunohistochemistry accounting for more than 10% of all cells were considered positive(+), otherwise negative (-). Progesterone receptor (PR) level was also examined to classify the tumors into two categories: PR negative (-) or PR positive (+). H3K27me3 was examined with anti-H3K27me3 (Millipore, 07-449) on ECL Plus films (Carestream).

MRI Image Acquisition

All patients underwent MRI scanning before operation (with or without Gadolinium enhancement). MRI scans were performed

by the Trio 3.0-T scanner (Siemens, Erlangen, Germany). The imaging process included axial T1WI (TE, 15 ms; TR, 450 ms; slice thickness, 5 mm), T2WI (TE, 110 ms; TR 5800 ms; slice thickness, 5 mm), and CE scans using 0.1 mM/kg gadopentetate dimeglumine (TE, 15 ms; TR, 450 ms; slice thickness, 5 mm). Tumor location was described according to AI-Mefty's published manuscript, such as parasagittal/falx, skull base, cerebral convexity, etc.

Tumor Segmentation and Feature Extraction

Preprocessing was performed using the 3D-Slicer software (version 4.11). The MRI DICOM files of all patients were imported into 3D-slicer. T1WI, T2Flair, and DWI images were registered to the T1c sequence images; N4 bias field correction was applied to each sequence image to correct non-uniformities in intensity. Two neuroradiologists painted regions of interest (ROIs) on T1c images using the 3D-slicer software. Multiple meningiomas from the same patient were considered as a single case in ROI classification and impact feature extraction. Enhancement of the dural tail sign was included in ROI, while peritumoral edema was excluded. The neuroradiologists were not informed of the clinical and biomarker data. Pyradiomics, an open-source python package (<https://github.com/Radiomics/pyradiomics>), was used to extract radiomic features.

Feature Selection and Establishment of Prediction Model

Pyradiomics, an open-source python package (<https://github.com/Radiomics/pyradiomics>), was used to extract radiomic features from the ROIs of each patient's images. After that, we eliminated the time, the checked hospital, machine model and other useless information. 130 radiomics features were retained in each sequence. To avoid degradation in model performance due to overfitting and increase in feature dimension, we evaluated radiomics features in distinguishing between mut/wild type and screened all radiomic features of each sequence to generate a new feature set.

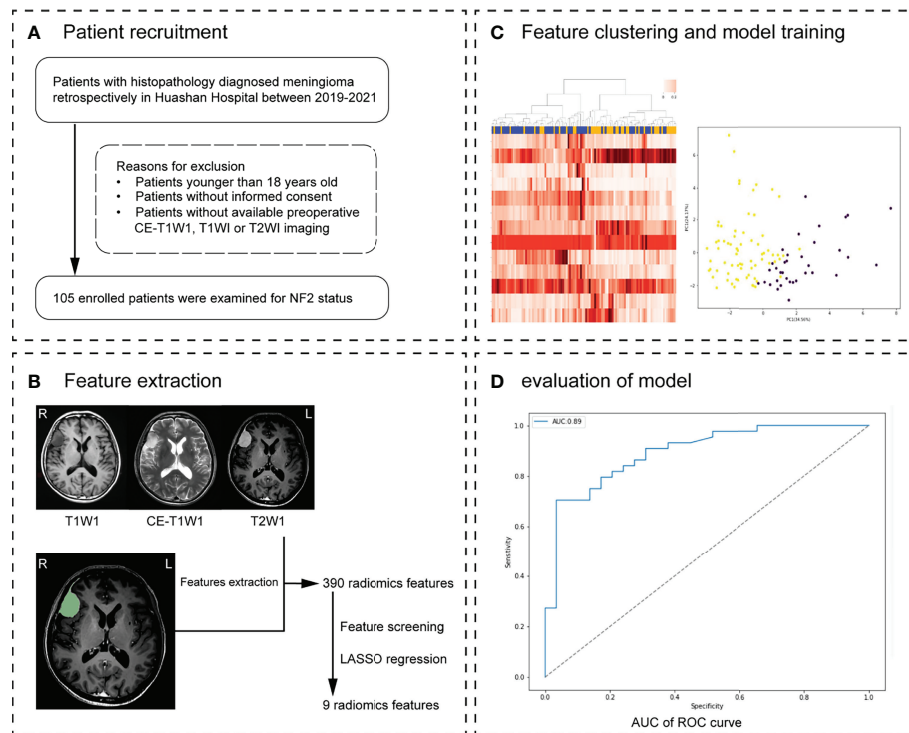


FIGURE 1 | Workflow. **(A)** Patient recruitment strategy. **(B)** 390 features were extracted from region of interest (ROI) on each magnetic resonance imaging (MRI) sequence. **(C)** The inner loop included hyperparameter tuning and features selection in the training datasets. After feature selection, the model with optimal parameters was used for prediction in the test set. This procedure developed 10 different models with specific sets of features and hyperparameters. **(D)** The effectiveness of the model was verified in the validation group. Receiver operating characteristic (ROC) analysis and precision and recall (P-R) analysis were used for model performance evaluation. The MRI scans of 30 meningioma patients from another hospital were used as external validation.

First, three pairs of samples in two groups were tested using t-test analysis. Levene test was used to test the homogeneity of variance. For the data with the homogeneity of variance greater than 0.05, a t-test was used to detect whether the characteristics of the average of the two groups of independent samples showed significant differences ($P < 0.05$). Only characteristics with significant differences were retained.

Second, a further feature screen was performed based on LASSO regression, which added L1 regular expression based on the least square regression. The features screened by t-test were standardized; the optimal parameter lambda was selected after ten-fold cross-validation. Thus, the corresponding coefficients of the model were trained. Features with nonzero coefficients in the LASSO regression model were selected.

Model Training and Evaluation

Machine learning models were developed to predict the outcome of NF2 status based on different algorithm. We used five supervised machine learning algorithms to establish the prediction model. All the cases were randomly divided into training and validation cohorts in the ratio of 7:3. The algorithm was trained based on the training group, and its effectiveness was verified in the validation group. The

algorithm with the highest AUC (area under the curve) in the validation cohorts was chosen as the best model. Five prediction models were generated by random forest (RF), k-nearest neighbor (KNN), support vector machine (SVM), logistic regression (LR), and extreme gradient boosting (xgboost) methods. The training and validation cohorts were divided based on the selected feature subset. Predictions were made after iterative optimization. The sensitivity, specificity, accuracy, and F1 score were evaluated. The model performance was analyzed by plotting ROC (receiver operating characteristic), P-R (analysis and precision-recall), and calibration curves. The MRI scans of 30 meningioma patients from First Affiliated Hospital of Nanjing Medical University were used as external validation to verify the accuracy of the best model.

Statistical Analysis

Statistical analysis was performed using SPSS 26.0 (IBM SPSS statistics 26.0 for mac; IBM corp). For continuous variables, the Student t-test was used; for comparison of mean values of continuous variables, ANOVA was used. Categorical variables were compared using the χ^2 test and the Fisher test. Continuous data were expressed as mean \pm SD. P-value < 0.05 was considered statistically significant.

RESULTS

Clinical Data and Immunohistochemistry

A total of 105 patients (32 males and 73 females) with intracranial meningiomas were recruited in the training and testing cohorts, including 60 patients with NF2 mutation/loss and 45 wild type patients. The mean age of the patients was 53.17 ± 9.60 years (range 31 to 73 years). There are 90 (85.71%) grade 1, 14 grade 2 (13.33%) and 1 grade 3 patients (0.95%), respectively. The most common pathological subtype was fibrous (45, 42.86%). The median Ki-67 labeling index was 3.91 ± 2.40 (range 1-12). PR was positive in 86 patients (81.9%). Loss of H3K27me3 expression was observed in 14 patients (13.3%). No difference was observed of the compared the clinical and immunohistochemical characteristics between NF2 mutant and wild-type groups. Parasinoidal (26/60) was the most common location in NF2 mut/loss group, while NF2 wild tumours were more likely in skull base locations (25/45). Three cases of multiple meningiomas were identified in our cohort. However, only one tumor in each patient was removed, which were all belonged to the NF2 mutation group. 16 patients (4 with wildtype NF2 and 12 with NF2 mutations) were regarded as recurrent meningiomas and no difference was observed between *de novo* and recurrent patients regarding NF2 status ($p = 0.170$).

NF2 Sequencing Analysis and LOH Analysis

Among all 105 patients, 52 patients (49.52%) had NF2 mutations; 8 patients (7.62%) showed loss of NF2 gene due to partial deletion of chromosome 22q. The remaining 45 patients had wild-type NF2. Allelic deletion of NF2 and mutations were classified as NF2 mutation group, amounting to 60 cases. Of all patients with NF2 mutations, 23 were nonsense mutations; 16 were frameshift mutation; 8 were splice site mutation; 4 were missense mutation. Exon 1 and Exon 6 was detected the highest mutation frequency, accounting for 6 (11.54%) and 7 (13.46%) of all mutants, respectively. However, we did not find any obvious hot spot mutations. The most common copy number deletion occurred in 22q11.21- q13.33. Details of the NF2 mutation status were shown in **Supplementary Table 1**.

Radiomic Feature Selection and Radiomic Signature Construction

A total of 130 radiomic features were extracted from each sequence. 390 radiomic features were included in the screening process. 147 radiomic features showed statistically significant differences between the NF2 mut/loss and wild-type groups. Only 9 features had nonzero coefficients in the LASSO regression model. The screening process of Lamda is shown in **Figure 2**. In **Figure 2A**, The red line represents the standard deviation of the mean square error (MSE) of λ . The blue bar indicates the range of the mean square error. The lambda with the lowest standard deviation is the most suitable for classification and the model is the simplest. Therefore, We chose the position with the lowest lambda standard deviation (red line) as the most appropriate λ Value. The details and p-values for these 9 features are shown in **Table 2**. 4 features were from the CE-T1Flair, 3 from T1WI, and 2 from T2WI sequences. 7 features could describe the texture of tumors and 2 described the wavelet of tumors. The 9 radiomics features were selected for the model building. We tried to cluster nine radiomics features through unsupervised hierarchical cluster analysis. PCA (Principal Component Analysis) is used to reduce the dimension and describe the distribution of data (**Figure 3**).

Finally, we decided to incorporate the 9 features into the model. Gray Level Dependence Matrix (GLDM) quantifies gray level dependencies in an image. included descriptors of the three-dimensional size and shape of the ROI. First-order statistics describe the distribution of voxel intensities within the image region defined by the mask through commonly used and basic metrics.

Gray Level Co-occurrence Matrix (GLCM) describes the second-order joint probability function of an image region constrained by the mask.

Model Training and Performance

We randomly divided all patients into training and validation groups in a ratio of 7:3. 73 patients were included in the training group. 9 radiomic features of 73 patients were used to train 5 supervised machine learning algorithms (RF, SVM, LR, KNN,

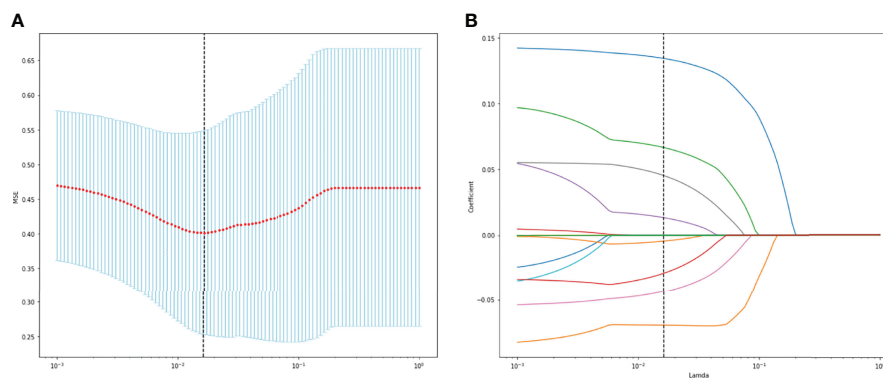


FIGURE 2 | (A) The change of MSE corresponding to the LASSO method. **(B)** Lamda value screening of LASSO regression.

TABLE 2 | The details of selected radiomics features.

| Name | Sequence | Type | p |
|---|----------|---------|-------|
| glcm_Imc2 | T2 | Texture | 0.027 |
| gldm_DependenceNonUniformity | T2 | Texture | 0.022 |
| shape_LeastAxisLength | T1 | Wavelet | 0.037 |
| firstorder_Minimum | T1 | Texture | 0.025 |
| glcm_ClusterShade | T1 | Texture | 0.037 |
| firstorder_Skewness | CET1 | Wavelet | 0.001 |
| glcm_JointAverage | CET1 | Texture | 0.005 |
| glcm_SumAverage | CET1 | Texture | 0.005 |
| gldm_LargeDependenceHighGrayLevelEmphasis | CET1 | Texture | 0.005 |

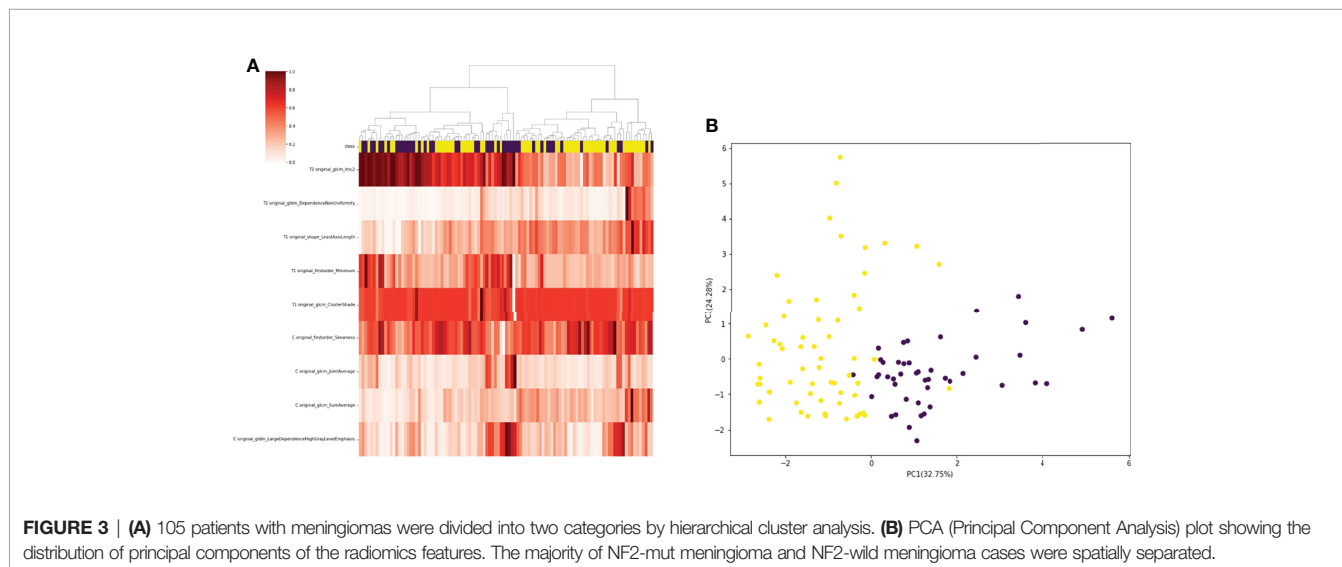
and xgboost). The data of a total of 32 patients in the validation cohort was used to evaluate the effectiveness of the algorithms. The AUCs of each algorithm in training and validation cohorts were calculated and compared as shown in **Table 3** and **Figure 4**. SVM (support vector machine) had the highest AUC of 0.89 in the training cohort and 0.85 in the validation cohort. F1 score is the harmonic average of accuracy and recall, while the value was 0.80 in the SVM model. LR (logistic regression) had an AUC of 0.84 in the training cohort and 0.82 in the validation cohort. Most of the algorithms had AUCs above 0.7.

Internal and External Verification

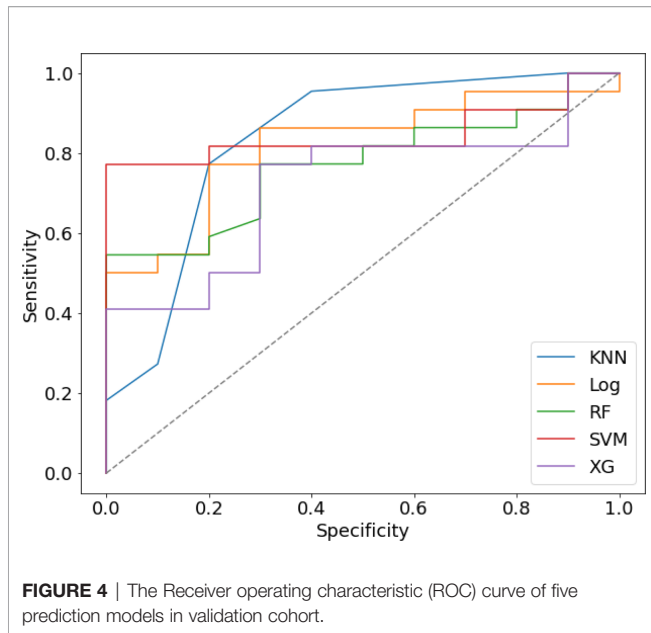
ROC and P-R curve analysis of SVM in training and validation cohorts were shown in **Figure 5**. AUC of SVM were 0.89 and 0.85 in the training cohort and validation cohort respectively. **Figure 6** shows the predicted value and their actual mutation of each validation group sample. Samples with a predicted value greater than 0 were predicted to be NF2 mut-type by the SVM model. The actual mutation of the sample were shown by color, Green represents mut-type and blue represents wild-type. 30 meningioma patients from First Affiliated Hospital of Nanjing Medical University were enrolled as external validation to verify the accuracy of the SVM model. the AUC of SVM model is 0.82 in the external validation cohorts. The calibration curve analysis and Hosmer-Lemeshow test for SVM model demonstrated the observations and predictions in validation cohorts were in good accordance (**Figure 7**).

DISCUSSION

NF2 inactivation was the most common alteration in meningiomas and played an important role in tumor

**TABLE 3** | The performances of five prediction models.

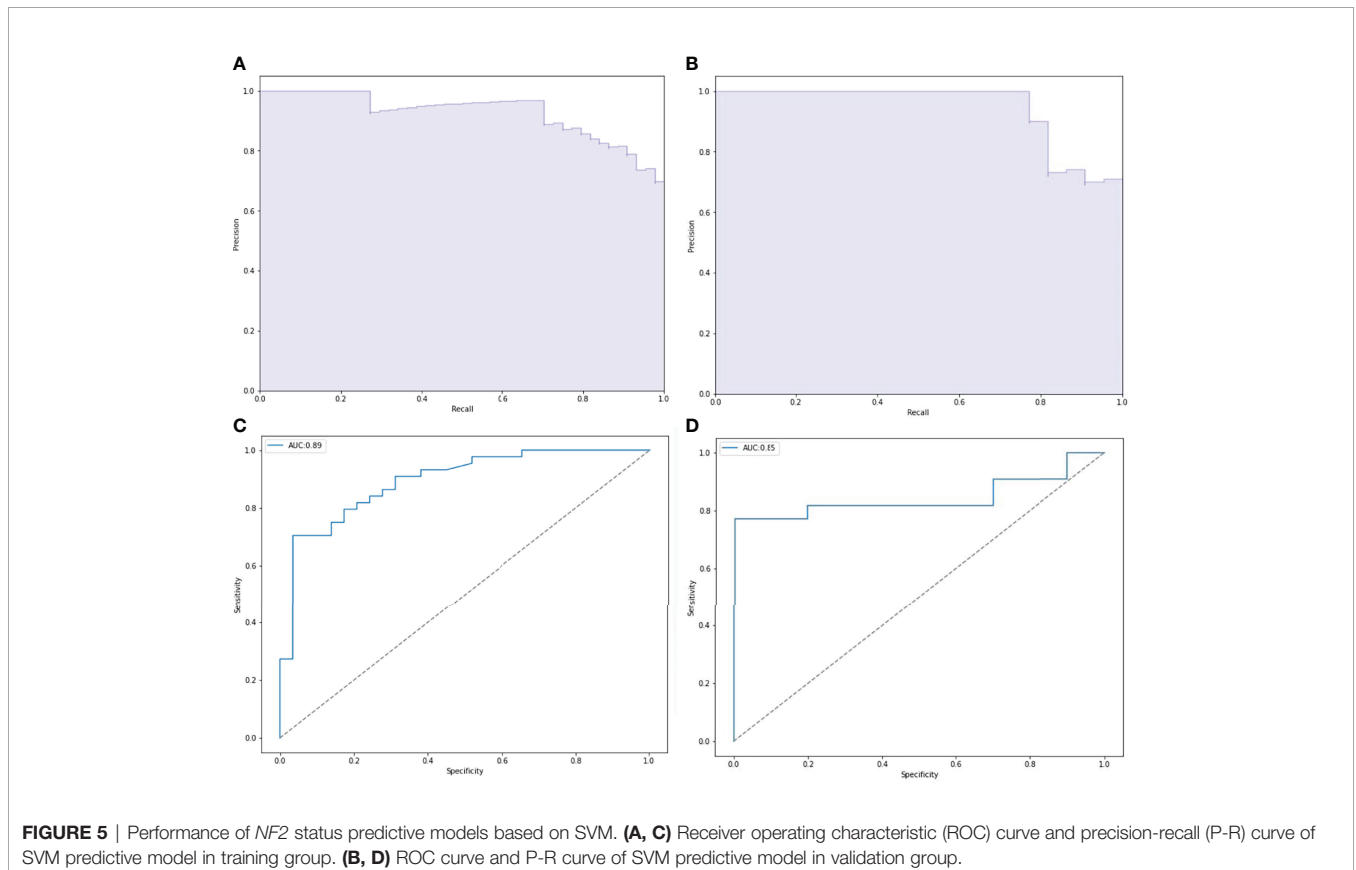
| Comparisons | Cohorts | LR | KNN | Xgboost | SVM | RF |
|-------------|---------|-------|-------|---------|-------|-------|
| AUC | train | 0.85 | 1 | 1 | 0.89 | 1 |
| | test | 0.85 | 0.76 | 0.82 | 0.85 | 0.77 |
| Sensitivity | train | 0.775 | 1 | 1 | 0.893 | 0.806 |
| | test | 0.75 | 0.692 | 0.74 | 0.7 | 0.6 |
| Specificity | train | 0.781 | 1 | 1 | 0.737 | 0.765 |
| | test | 0.8 | 0.789 | 0.88 | 0.727 | 0.765 |
| Accuracy | train | 0.779 | 1 | 1 | 0.779 | 0.779 |
| | test | 0.781 | 0.751 | 0.78 | 0.71 | 0.688 |
| F1-score | train | 0.729 | 1 | 1 | 0.685 | 0.716 |
| | test | 0.72 | 0.692 | 0.76 | 0.609 | 0.643 |



progression (5, 18). Given this, the prediction of *NF2* inactivation status before surgery might be meaningful for determining an appropriate personalized treatment strategy. In this study, we built a machine learning model to preoperatively predict the

status of *NF2* inactivation by radiomic analysis. We observed that the models based on SVM produced excellent results in the machine-learning experiments. Our radiomics model may aid the early identification of meningioma patients with *NF2* mutation.

NF2 is located on the long arm of chromosome 22 (chr22q) and encodes a 69 kDa protein named merlin (moesin-ezrin-radixin-like protein). *NF2* is a member of the Band 4.1 FERM gene family (19). Merlin plays important role in several essential pathways, including HIPPO pathway, mTOR/PI3K/AKT pathway, and receptor tyrosine kinases (RTKs) (20, 21). Previous studies showed that more than 60% of sporadic meningioma patients harbored somatic mutation, epigenetic inactivation, or allele loss of *NF2* on chr22q. The proportion is even higher in high-grade meningiomas (22–24). In a study of 88 sporadic meningiomas, 49% exhibited allelic loss of chromosome 22, 24% had *NF2* somatic mutations and 26% had aberrant *NF2* promoter methylation. In 17% of the meningiomas, epigenetic *NF2* inactivation was the only cause of *NF2* deficiency (24). Compared to *NF2*-wt meningioma, *NF2* mutant meningiomas was detected with a higher proliferation index (Ki-67 labels) and often manifested in comparatively larger tumor size (25). In addition, the deletion of *NF2* leads to overexpression of focal adhesion kinase (FAK), resulting in enhanced cell migration and invasion (26). In all, non-invasive preoperative prediction of *NF2* mutation might be of use. The knowledge of *NF2* status might



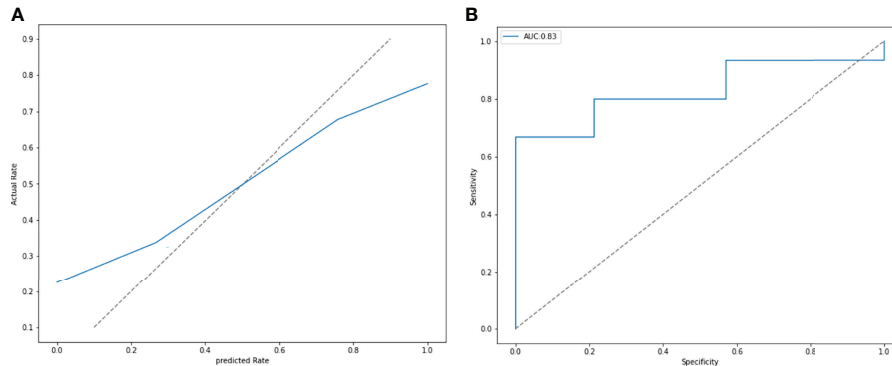


FIGURE 6 | (A) The calibration curve analysis and Hosmer-Lemeshow test for SVM model demonstrated the observations and predictions in validation cohorts were in good accordance. ($P = 0.411$). **(B)** External validation was performed by 30 patients from other hospitals. The SVM model had an AUC of 0.83.

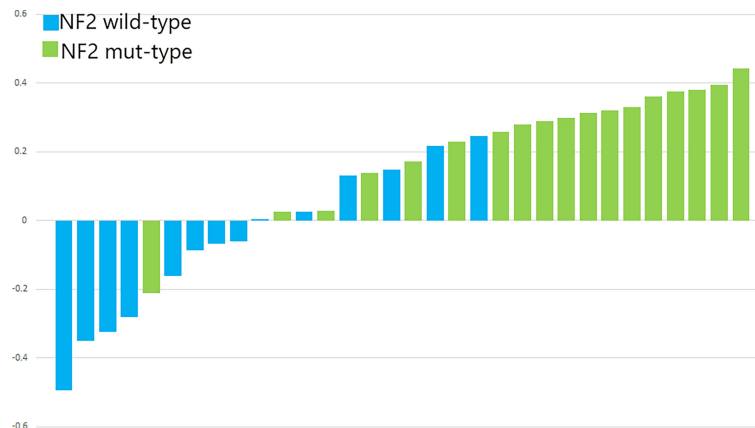


FIGURE 7 | The p-values of SVM for the validation cohorts. The blue bars show the radiomics signature values for the *NF2*-wild meningiomas, and the green bars show the values for the *NF2*-mut meningiomas.

play a role in decision making of appropriate clinical treatment strategies for meningioma patients.

Recently, several studies on radiomics focused on meningiomas and demonstrated encouraging results. Previous studies could distinguish WHO grade I meningiomas out of WHO grade II and III meningiomas by radiomic analysis models. These models were proved to have high accuracy and sensitivity (27, 28). Lei et al. distinguished two subtypes in WHO grade I meningiomas by radiomics with an accuracy higher than 90% (29). Other studies focused on predicting clinical characteristics of meningiomas, such as extent of peritumoral edema and tumor consistency. For example, Bing et al. analyzed peritumoral edema in meningioma patients using an SVM-based machine learning algorithm combined with clinical data (14). Zhai et al. constructed a radiomic-based signature to predict meningioma consistency with AUC of 0.94 in the validation cohort (13). Taken together, previous studies proved the feasibility of radiomic analysis for meningioma imaging. Some

studies also predicted the molecular typing of other primary tumors, such as breast cancer and glioma. Monti et al. extracted quantitative radiomic features from DCE-MRI pharmacokinetic data to differentiate ER, PR, and HER2 status in breast cancer (30). In glioma, radiomics had been used to predict IDH mutation and co-deletion of 1p/19q (31, 32). However, up to now, the report of such studies on meningiomas is scarce.

In this study, we first detected the occurrence of *NF2* inactivation in the tumor samples. Mutations or loss of *NF2* gene were also considered as inactivation of *NF2*. By feature extraction and screening, we finally obtained 9 significant radiomic features. In previous studies, screening features of meningiomas ranged between 3 to 22 (27–29). The discrepancy might be attributed to difference in the process of screening and imaging data heterogeneity. Most of the 9 features were extracted from T1WI plain scan and Gadolinium enhanced sequences (33). The AUC of linear model based on SVM was 0.85 and 0.82 in the internal and external validation cohorts

respectively, consistent with findings of other studies which predicted intracranial tumor biomarkers (31, 32). There were many radiomics studies involving HER2 in breast cancers and IDH1 in gliomas (34, 35). Approximately, 70% of HER2 mutations occurred between amino acids 755 and 781 (exons 19 and 20) in breast cancers (36). 80% of IDH1 mutations in gliomas occurred on R132H (37). *NF2* has 17 exons and harbors no significant hotspot mutations (21). Our cohorts also showed no significant hotspot mutations, in accordance to previous reports. This may affect our prediction results; however, we found AUCs for most of our models were above 0.7 in the validation cohort. The data was not sufficient enough to distinguish the differences between *NF2* mutation types.

In our cohort, multiple meningiomas in a single patient were considered as one tumor in ROI selection and feature extraction. That's because they chose to remove only the symptomatic meningioma. Somatic mutation of *NF2* is related to neurofibromatosis type 2 (38) and is often found in multiple intracranial meningiomas. All our 3 cases of multiple meningiomas belonged to the *NF2* mutation group. Whereas, the difference in number of multiple meningiomas between *NF2* mutant and wild-type groups had no statistical significance. *NF2* plays an important role in progression of meningiomas (39). Additionally, there was no significant difference in number of relapse patients between the two groups, The limitations mentioned above might be attributed to the comparatively small sample size. A study by Clark et al. reported that in meningiomas with *NF2*- mutations, tumor location had a predilection for the posterior and lateral skull base, tentorium, and cerebral falx, while sporadic mutations, such as those in *TRAF7* and *SMO*, tended to be relevant with anterior skull base location (5). This phenomenon was not observed in our cohort. In some previous studies, clinical data were added to radiomic models to optimize the impact (14). No significant clinical features were found in our cohort, so these were not included in the analysis.

Recently, radiomics studies of other diseases selected ROI through automatic segmentation, such as lung cancer, breast cancer and gastric disease (40–42). Jonathan et al. had developed an algorithm based on convolutional neural network to automatically segment vestibular schwannoma and achieved satisfactory results (43). The application of automatic segmentation could benefit our research and clinical practice. Although at present, no research showed that there is a difference in accuracy between automatic segmentation and manual segmentation. Some studies showed that there was no meningioma tumor cell in the gadolinium enhanced meningeal tail sign (44), while some others drew the opposite conclusion (45). We included the meningeal tail sign in ROI analysis because the boundary between the meningeal tail sign and meningioma is difficult to distinguish.

There were limitations in our present study. First, this was a retrospective study with comparatively small sample size which could have limited the accuracy of our model. Probably due to restriction of sample size, many difference in clinical and immunohistochemical features showed no statistical significance. Second, the result of this study predicts binary

variables. All our radiomic algorithms were based on linear models. There might be nonlinear models with a higher fitting degree. Finally, the clinical follow-up of these patients is still underway. Hopefully, the follow-up data might further confirm the significance of preoperative prediction of *NF2* status.

CONCLUSION

This retrospective study demonstrated that multiparametric MRI-based radiomics analysis could be a promising approach for preoperative prediction of *NF2* inactivation in patients with meningioma. It could serve as an effective non-invasive approach to predict *NF2* inactivation and help determine individualized therapeutic regime for patients with meningioma.

DATA AVAILABILITY STATEMENT

The original contributions presented in the study are publicly available. This data can be found here: <https://www.ncbi.nlm.nih.gov/sra, PRJNA858222>.

ETHICS STATEMENT

Written informed consent was obtained from the individual(s) for the publication of any potentially identifiable images or data included in this article.

AUTHOR CONTRIBUTIONS

SS prepared the first version of the editorial. LR, ZM, LH and YG discuss the editorial content and revised the final editorial text. All authors contributed to the article and approved the submitted version.

ACKNOWLEDGMENTS

This study was supported by grants from the National Natural Science Foundation of China (82072788 to YG, 82203390 to LYH and 82203204 to JJD), the Science and Technology Commission of Shanghai Municipality (22140900200 to YG) and Shanghai Sailing Program (20YF1403900 to LYH).

SUPPLEMENTARY MATERIAL

The Supplementary Material for this article can be found online at: <https://www.frontiersin.org/articles/10.3389/fonc.2022.879528/full#supplementary-material>

REFERENCES

- Preusser M, Brastianos P, Mawrin C. Advances in Meningioma Genetics: Novel Therapeutic Opportunities. *Nat Rev Neurol* (2018) 14(2):106–15. doi: 10.1038/nrnneurol.2017.168
- Ostrom Q, Patil N, Cioffi G, Waite K, Kruchko C, Barnholtz-Sloan J. CBTRUS Statistical Report: Primary Brain and Other Central Nervous System Tumors Diagnosed in the United States in 2013–2017. *Neuro-oncology* (2020) 22:iv1–iv96. doi: 10.1093/neuonc/noaa200
- Whittle I, Smith C, Navoo P, Collie D. Meningiomas. *Lancet (London England)* (2004) 363(9420):1535–43. doi: 10.1016/s0140-6736(04)16153-9
- Riemenschneider M, Perry A, Reifenberger G. Histological Classification and Molecular Genetics of Meningiomas. *Lancet Neurol* (2006) 5(12):1045–54. doi: 10.1016/s1474-4422(06)70625-1
- Clark V, Erson-Omay E, Serin A, Yin J, Cotney J, Ozduman K, et al. Genomic Analysis of non-NF2 Meningiomas Reveals Mutations in TRAF7, KLF4, AKT1, and SMO. *Sci (New York NY)* (2013) 339(6123):1077–80. doi: 10.1126/science.1233009
- Brastianos P, Horowitz P, Santagata S, Jones R, McKenna A, Getz G, et al. Genomic Sequencing of Meningiomas Identifies Oncogenic SMO and AKT1 Mutations. *Nat Genet* (2013) 45(3):285–9. doi: 10.1038/ng.2526
- Youngblood M, Miyagishima D, Jin L, Gupte T, Li C, Duran D, et al. Associations of Meningioma Molecular Subgroup and Tumor Recurrence. *Neuro Oncol* (2021) 23(5):783–94. doi: 10.1093/neuonc/noaa226
- Lambin P, Rios-Velazquez E, Leijenaar R, Carvalho S, van Stiphout R, Granton P, et al. Radiomics: Extracting More Information From Medical Images Using Advanced Feature Analysis. *Eur J Cancer (Oxford Engl 1990)* (2012) 48(4):441–6. doi: 10.1016/j.ejca.2011.11.036
- Liu Z, Wang S, Dong D, Wei J, Fang C, Zhou X, et al. The Applications of Radiomics in Precision Diagnosis and Treatment of Oncology: Opportunities and Challenges. *Theranostics* (2019) 9(5):1303–22. doi: 10.7150/thno.30309
- Li Z, Kaiser L, Holzgreve A, Ruf V, Suchorska B, Wenter V, et al. Prediction of TERTp-Mutation Status in IDH-Wildtype High-Grade Gliomas Using Pre-Treatment Dynamic [F]FET PET Radiomics. *Eur J Nucl Med Mol Imaging* (2021) 48(13):4415–25. doi: 10.1007/s00259-021-05526-6
- Langenhuizen P, Zinger S, Leenstra S, Kunst H, Mulder J, Hanssens P, et al. Radiomics-Based Prediction of Long-Term Treatment Response of Vestibular Schwannomas Following Stereotactic Radiosurgery. *Otology Neurotology* (2020) 41(10):e1321–7. doi: 10.1097/mao.0000000000002886
- Khanna O, Fathi Kazerooni A, Farrell C, Baldassari M, Alexander T, Karsy M, et al. Machine Learning Using Multiparametric Magnetic Resonance Imaging Radiomic Feature Analysis to Predict Ki-67 in World Health Organization Grade I Meningiomas. *Neurosurgery* (2021) 89(5):928–36. doi: 10.1093/neuros/nyab307
- Zhai Y, Song D, Yang F, Wang Y, Jia X, Wei S, et al. Preoperative Prediction of Meningioma Consistency via Machine Learning-Based Radiomics. *Front Oncol* (2021) 11:657288. doi: 10.3389/fonc.2021.657288
- Xiao B, Fan Y, Zhang Z, Tan Z, Yang H, Tu W, et al. Three-Dimensional Radiomics Features From Multi-Parameter MRI Combined With Clinical Characteristics Predict Postoperative Cerebral Edema Exacerbation in Patients With Meningioma. *Front Oncol* (2021) 11:625220. doi: 10.3389/fonc.2021.625220
- Liu X, Li Y, Li S, Fan X, Sun Z, Yang Z, et al. IDH Mutation-Specific Radiomic Signature in Lower-Grade Gliomas. *Aging* (2019) 11(2):673–96. doi: 10.18632/aging.101769
- Li Y, Qian Z, Xu K, Wang K, Fan X, Li S, et al. MRI Features Predict P53 Status in Lower-Grade Gliomas via a Machine-Learning Approach. *NeuroImage Clin* (2018) 17:306–11. doi: 10.1016/j.nicl.2017.10.030
- Deng J, Sun S, Chen J, Wang D, Cheng H, Chen H, et al. TERT Alterations Predict Tumor Progression in High-Grade Meningiomas Following Adjuvant Radiotherapy. *Front Oncol* (2021) 11:747592. doi: 10.3389/fonc.2021.747592
- Birzu C, Peyre M, Sahn F. Molecular Alterations in Meningioma: Prognostic and Therapeutic Perspectives. *Curr Opin Oncol* (2020) 32(6):613–22. doi: 10.1097/cco.0000000000000687
- Asthaigiri A, Parry D, Butman J, Kim H, Tsilou E, Zhuang Z, et al. Neurofibromatosis Type 2. *Lancet (London England)* (2009) 373(9679):1974–86. doi: 10.1016/s0140-6736(09)60259-2
- Stamenkovic I, Yu Q. Merlin, a "Magic" Linker Between Extracellular Cues and Intracellular Signaling Pathways That Regulate Cell Motility, Proliferation, and Survival. *Curr Protein Pept Sci* (2010) 11(6):471–84. doi: 10.2174/138920310791824011
- Petrilli A, Fernández-Valle C. Role of Merlin/NF2 Inactivation in Tumor Biology. *Oncogene* (2016) 35(5):537–48. doi: 10.1038/ncr.2015.125
- Ruttledge M, Sarrazin J, Rangaratnam S, Phelan C, Twist E, Merel P, et al. Evidence for the Complete Inactivation of the NF2 Gene in the Majority of Sporadic Meningiomas. *Nat Genet* (1994) 6(2):180–4. doi: 10.1038/ng0294-180
- Gutmann D, Giordano M, Fishback A, Guha A. Loss of Merlin Expression in Sporadic Meningiomas, Ependymomas and Schwannomas. *Neurology* (1997) 49(1):267–70. doi: 10.1212/wnl.49.1.267
- Lomas J, Bello M, Arjona D, Alonso M, Martínez-Glez V, López-Marín I, et al. Genetic and Epigenetic Alteration of the NF2 Gene in Sporadic Meningiomas. *Genes Chromosomes Cancer* (2005) 42(3):314–9. doi: 10.1002/gcc.20141
- Yuzawa S, Nishihara H, Yamaguchi S, Mohri H, Wang L, Kimura T, et al. Clinical Impact of Targeted Amplicon Sequencing for Meningioma as a Practical Clinical-Sequencing System. *Modern Pathol* (2016) 29(7):708–16. doi: 10.1038/modpathol.2016.81
- Abedalthagafi M, Bi W, Aizer A, Merrill P, Brewster R, Agarwalla P, et al. Oncogenic PI3K Mutations are as Common as AKT1 and SMO Mutations in Meningioma. *Neuro Oncol* (2016) 18(5):649–55. doi: 10.1093/neuonc/nov316
- Hamerla G, Meyer H, Schob S, Ginat D, Altman A, Lim T, et al. Comparison of Machine Learning Classifiers for Differentiation of Grade 1 From Higher Grading in Meningioma: A Multicenter Radiomics Study. *Magnetic Resonance Imaging* (2019) 63:244–9. doi: 10.1016/j.mri.2019.08.011
- Zhu Y, Man C, Gong L, Dong D, Yu X, Wang S, et al. A Deep Learning Radiomics Model for Preoperative Grading in Meningioma. *Eur J Radiol* (2019) 116:128–34. doi: 10.1016/j.ejrad.2019.04.022
- Niu L, Zhou X, Duan C, Zhao J, Sui Q, Liu X, et al. Differentiation Researches on the Meningioma Subtypes by Radiomics From Contrast-Enhanced Magnetic Resonance Imaging: A Preliminary Study. *World Neurosurg* (2019) 126:e646–52. doi: 10.1016/j.wneu.2019.02.109
- Monti S, Aiello M, Incoronato M, Grimaldi A, Moscarino M, Mirabelli P, et al. DCE-MRI Pharmacokinetic-Based Phenotyping of Invasive Ductal Carcinoma: A Radiomic Study for Prediction of Histological Outcomes. *Contrast Media Mol Imaging* (2018) 2018:5076269. doi: 10.1155/2018/5076269
- Kim M, Jung S, Park J, Jo Y, Park S, Nam S, et al. Diffusion- and Perfusion-Weighted MRI Radiomics Model may Predict Isocitrate Dehydrogenase (IDH) Mutation and Tumor Aggressiveness in Diffuse Lower Grade Glioma. *Eur Radiol* (2020) 30(4):2142–51. doi: 10.1007/s00330-019-06548-3
- Casale R, Lavrova E, Sanduleanu S, Woodruff H, Lambin P. Development and External Validation of a non-Invasive Molecular Status Predictor of Chromosome 1p/19q Co-Deletion Based on MRI Radiomics Analysis of Low Grade Glioma Patients. *Eur J Radiol* (2021) 139:109678. doi: 10.1016/j.ejrad.2021.109678
- Elster A, Challa V, Gilbert T, Richardson D, Contento J. Meningiomas: MR and Histopathologic Features. *Radiology* (1989) 170:857–62. doi: 10.1148/radiology.170.3.2916043
- Pirozzi C, Yan H. The Implications of IDH Mutations for Cancer Development and Therapy. *Nat Rev Clin Oncol* (2021) 18(10):645–61. doi: 10.1038/s41571-021-00521-0
- Loibl S, Poortmans P, Morrow M, Denkert C, Curigliano G. Breast Cancer. *Lancet (London England)* (2021) 397(10286):1750–69. doi: 10.1016/s0140-6736(20)32381-3
- Cocco E, Lopez S, Santin AD, Scaltriti M. Prevalence and Role of HER2 Mutations in Cancer. *Pharmacol Ther* (2019) 199:188–96. doi: 10.1016/j.pharmthera.2019.03.010
- Dang L, Yen K, Attar E. IDH mutations in cancer and progress toward development of targeted therapeutics. *Ann Oncol: Official J Eur Surg Med Oncol* (2016) 27(4):599–608. doi: 10.1093/annonc/mdw013
- Evans D. Neurofibromatosis Type 2 (NF2): A Clinical and Molecular Review. *Orphanet J Rare Diseases* (2009) 4:16. doi: 10.1186/1750-1172-4-16
- Sahn F, Schrimpf D, Stichel D, Jones D, Hielscher T, Schefzyk S, et al. DNA Methylation-Based Classification and Grading System for Meningioma: A

- Multicentre, Retrospective Analysis. *Lancet Oncol* (2017) 18(5):682–94. doi: 10.1016/s1470-2045(17)30155-9
40. Liu X, Li K, Yang R, Geng L. Review of Deep Learning Based Automatic Segmentation for Lung Cancer Radiotherapy. *Front Oncol* (2021) 11:717039. doi: 10.3389/fonc.2021.717039
41. Chen X, Men K, Chen B, Tang Y, Zhang T, Wang S, et al. CNN-Based Quality Assurance for Automatic Segmentation of Breast Cancer in Radiotherapy. *Front Oncol* (2020) 10:524. doi: 10.3389/fonc.2020.00524
42. Tan J, Wang L, Chen Y, Xi W, Ji J, Wang L, et al. Predicting Chemotherapeutic Response for Far-Advanced Gastric Cancer by Radiomics With Deep Learning Semi-Automatic Segmentation. *J Cancer* (2020) 11(24):7224–36. doi: 10.7150/jca.46704
43. Shapay J, Kujawa A, Dorent R, Wang G, Dimitriadis A, Grishchuk D, et al. Segmentation of Vestibular Schwannoma From MRI, an Open Annotated Dataset and Baseline Algorithm. *Sci Data* (2021) 8(1):286. doi: 10.1038/s41597-021-01064-w
44. Tokumaru A, Ouchi T, Eguchi T, Kawamoto S, Kokubo T, Suzuki M, et al. Prominent Meningeal Enhancement Adjacent to Meningioma on Gd-DTPA-Enhanced MR Images: Histopathologic Correlation. *Radiology* (1990) 175(2):431–3. doi: 10.1148/radiology.175.2.2326470
45. Rokni-Yazdi H, Azmoudeh Ardalan F, Asadzandi Z, Sotoudeh H, Shakiba M, Adibi A, et al. Pathologic Significance of the "Dural Tail Sign". *Eur J Radiol* (2009) 70(1):10–6. doi: 10.1016/j.ejrad.2008.01.010

Conflict of Interest: The authors declare that the research was conducted in the absence of any commercial or financial relationships that could be construed as a potential conflict of interest.

Publisher's Note: All claims expressed in this article are solely those of the authors and do not necessarily represent those of their affiliated organizations, or those of the publisher, the editors and the reviewers. Any product that may be evaluated in this article, or claim that may be made by its manufacturer, is not guaranteed or endorsed by the publisher.

Copyright © 2022 Sun, Ren, Miao, Hua, Wang, Deng, Chen, Liu and Gong. This is an open-access article distributed under the terms of the Creative Commons Attribution License (CC BY). The use, distribution or reproduction in other forums is permitted, provided the original author(s) and the copyright owner(s) are credited and that the original publication in this journal is cited, in accordance with accepted academic practice. No use, distribution or reproduction is permitted which does not comply with these terms.